# Phase Behavior and Microstructure of Microemulsions with a Room-Temperature Ionic Liquid as the Polar Phase

**Rob Atkin*,† and Gregory G. Warr**

*School of Chemistry, Building F11, The University of Sydney, NSW 2006, Australia*

*Received: August 4, 2006; In Final Form: March 7, 2007*

Microemulsions of nonionic alkyl oligoethyleneoxide ($C_iE_j$) surfactants, alkanes, and ethylammonium nitrate (EAN), a room-temperature ionic liquid, have been prepared and characterized. Studies of phase behavior reveal that EAN microemulsions have many features in common with corresponding aqueous systems, the primary difference being that higher surfactant concentrations and longer surfactant tailgroups are required to offset the decreased solvophobicity the surfactant molecules in EAN compared with water. The response of the EAN microemulsions to variation in the length of the alkane, surfactant headgroup, and surfactant tailgroup has been found to parallel that observed in aqueous systems in most instances. EAN microemulsions exhibit a single broad small-angle X-ray scattering peak, like aqueous systems. These are well described by the Teubner−Strey model. A lamellar phase was also observed for surfactants with longer tails at lower temperatures. The scattering peaks of both microemulsion and lamellar phases move to lower wave vector on increasing temperature. This is ascribed to a decrease in the interfacial area of the surfactant layer. Phase behavior, small-angle X-ray scattering, and conductivity experiments have allowed the weakly to strongly structured transition to be identified for EAN systems.

## Introduction

Room-temperature ionic liquids (ILs) are currently attracting considerable scientific interest on several fronts. ILs are "green solvents" due to their low vapor pressure, and "designer solvents" because their physical properties can be varied predictably by incorporation of appropriate functional groups.[1−3] ILs solubilize many organic and inorganic species facilitating reactions between unusual combinations of reagents. Both hydrophilic and hydrophobic ILs that are immiscible with oil and water, respectively, have been identified.[4] Self-assembly of surfactants into micelles has been reported in a variety of ILs.[5,6] Recently, a range of liquid crystalline phases,[7] and adsorbed surfactant aggregates on graphite,[8] have been identified for alkyl oligoethyleneoxide ($C_iE_j$) surfactants in ethylammonium nitrate (EAN), a protic IL with the capacity to form a hydrogen-bonding network.[9] In this study we report the phase behavior of ternary mixtures of these surfactants, oil and EAN, and the structure and stability of the microemulsion phases thus formed as a function of surfactant concentration and temperature.

Traditional microemulsions are thermodynamically stable, nanostructured mixtures of water and oil stabilized by surfactants, and in some cases, co-surfactants. They are optically transparent, usually have low viscosity, and are widely used in a variety of formulations.[10] The monomolecular film of surfactant molecules that separate immiscible polar and nonpolar solvents in a microemulsion impart a spreading pressure that reduces the interfacial tension. When this interfacial tension approaches zero, a bicontinous microemulsion may form, in which surfactant monolayers separate disordered, interpenetrating domains of oil and water.[11] Undulations in the monolayer are controlled by the curvature energies,[12] described by the bending modulus, saddle-splay modulus and spontaneous curvature of the surfactant film.[13] The physical properties of microemulsions are often investigated using nonionic $C_iE_j$ surfactants, as their structure is readily varied systematically and film curvature may be altered by simply changing temperature. This permits relatively straightforward and systematic investigation of the structures formed.[14]

Several recent papers have reported novel microemulsions where an IL is substituted for the water or oil phase. A microemulsion of 1-butyl-3-methylimidazolium tetrafluoroborate ($bmimBF_4$) and cyclohexane stabilized by the nonionic surfactant, Triton X-100, has been prepared and characterized.[15] Freeze-fracture electron microscopy suggested that the microemulsion phase consisted of droplets of IL in cyclohexane at 35 °C, and small angle neutron scattering showed that the microemulsion droplets could be swollen by the addition of IL.[16] This study reported that much higher concentrations of surfactant were required to stabilize the IL microemulsion than for similar aqueous systems. Microemulsions consisting of water and a hydrophobic IL, 1-butyl-3-methylimidazolium hexafluorophosphate, stabilized using TX-100 and Tween 20 have also been reported.[17,18] The ternary phase behavior of IL microemulsions is, however, relatively poorly understood, and the structural variation within the microemulsion phase as a function of surfactant concentration and temperature is unknown. This study aims to elucidate these issues using studies of phase behavior with the microstructure of the solution determined using small-angle X-ray scattering (SAXS).

The phase behavior of self-assembling ternary mixtures is often studied as a function of temperature and composition by taking "slices" through the phase prism at a 1 to 1 oil to water ratio while varying the surfactant concentration. The phase boundaries give rise to a characteristic "fish" outline[14,19] (shown schematically in Figure 1) frequently reported by Kahlweit, Strey, and co-workers for water-based microemulsions. For a thorough explanation of the origin of the microemulsion phase

* Corresponding author phone: +61 2 49217107; fax: +61 2 49215472; e-mail: rob.atkin@newcastle.edu.au.

† Current address: Chemistry Building, The University of Newcastle, Callaghan, NSW 2308, Australia.

10.1021/jp065020n CCC: $37.00 
Published on Web 07/17/2007

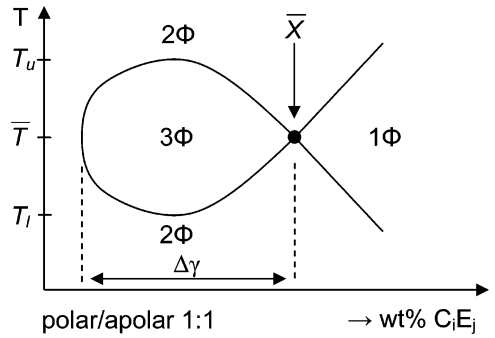


**Figure 1.** Schematic fish-shaped phase diagram obtained by taking a vertical section through the phase prism for equal masses of polar and apolar solvent, showing single phase (1Φ), two phase and three phase regions. For other symbols, see text.

for nonionic surfactants, water and oil, the reader is directed to refs 14 and 19 (and references therein). Briefly, the three-phase state that may form in ternary mixtures, in which the middle phase is a microemulsion, results from miscibility gaps in the three binary systems: water−surfactant, water−oil, and oil-surfactant. At low temperatures, the surfactant is dissolved in the aqueous phase, and oil-swollen micelles form, with an upper phase of excess oil. At high temperatures, oil is a superior solvent for the surfactant, and water-swollen reverse micelles form in an oil continuous phase, in equilibrium with a lower phase of excess water. At intermediate temperatures, the surfactant has high solubility in both water and oil. This produces a surfactant-rich middle phase in equilibrium with excess oil and water.

The dimensions and position of the three-phase body define the characteristic values of a microemulsion system, as shown in Figure 1. The maximum temperature interval over which the three phases occur is defined as $\Delta T = T_u - T_l$, where $T_u$ and $T_l$ are the maximum and minimum temperatures at which the three phases appear, respectively.[19] At the mean temperature, $\bar{T}$, the efficiency of the surfactant in dissolving both water and oil is maximized. As the surfactant concentration is increased, the surfactant-rich middle phase increases in volume, eventually producing a single phase. At this position in the phase diagram, $\bar{X}$, the microemulsion is said to be balanced, with zero mean curvature of the surfactant film, and the bicontinous microemulsion forms. $\bar{X}$ thus defines surfactant efficiency, which is the minimum surfactant concentration required to solubilize the two immiscible solvents. $\bar{T}$ is also defined as the phase inversion temperature.

In aqueous systems, $\bar{T}$ is determined by the interplay between the lower consolute temperature ($T_\beta$) in the binary water−surfactant system (the cloud point), and the upper consolute temperature ($T_\alpha$) in the binary oil−surfactant system.[19] $T_\alpha$ and $T_\beta$ change in a predictable fashion with variation in the system parameters $i$ (number of $CH_2$ units in the tailgroup), $j$ (number of ethoxy units in the headgroup), and $k$ (number of $CH_2$ units in the alkane solvent). It has previously been shown that *binary* $C_iE_j$−EAN systems have many features in common with aqueous systems including, critically for this work, cloud points, $T_\beta$.[7] This study will examine whether variation in surfactant and alkane structure ($i$, $j$, and $k$) produces corresponding effects for microemulsions in which the polar phase is an ionic liquid, EAN.

## Materials and Methods

99% pure alkyl oligoethyleneoxide surfactants were obtained from BioChemika and used without further purification. >99% pure octane, decane, dodecane, tetradecane, and hexadecane were obtained from Aldrich and used without further purification.

EAN (M.P. = 12 °C) was prepared by reacting equimolar amounts of ethylamine and concentrated nitric acid to produce an aqueous solution, as described by Evans et al.[5] Excess water was removed by first purging the EAN solution with nitrogen, then heating it at 110−120 °C for several hours under a nitrogen atmosphere. This leads to water contents undetectable by Karl Fischer titration (<0.01%) and prevents the formation of nitrous oxide impurities that, if present, produce a yellow discoloration.

Phase diagrams were determined by weighing known amounts of surfactant into sample tubes and adding oil and EAN in a 1:1 mass ratio such that the total sample mass was 1 gram. These samples were equilibrated at temperatures between 5 and ∼70 °C in a water bath (±0.1 °C), and the number of phases present was recorded. This allows the boundaries of the three-phase body to be determined. 70 °C was the practical upper temperature limit, as above this temperature the aforementioned nitrous oxide impurities develop over time in EAN. Samples were generally equilibrated for at least 24 h at each temperature because phases in these IL systems tended to separate very slowly. As a result, we estimate the error in the position of the phase boundaries to be on the order of 1−2 °C. In some systems, particularly at low temperatures, the formation of a stable macroemulsion at the interface between phases hindered determination of the position of the phase boundaries. These emulsions were dispersed by heating them to ∼70 °C, after which they were cooled over several days. Even so, the errors associated with these points are significantly higher, so regions of the phase diagram where this occurred are shaded gray in Figures 3 and 4.

SAXS experiments were carried out on a Bruker Nanostar equipped with a rotating anode source (Cu Kα, 1.541 Å), cross-coupled Göbel mirrors, three-pinhole collimation, and Hi-Star 2D detector with 100 μm resolution, situated at ANSTO Lucas Heights. The available $q$-range for the experiments was 0.015−0.22 $Å^{-1}$, which was not sufficiently high to enable a Porod analysis of the internal interface. Samples were sealed in glass capillaries of 2 mm diameter with 0.1 mm wall thickness. The sample and camera environments were evacuated prior to measurement to prevent background scattering by air. The typical measuring times were between 20 min and 1 h with temperature stability of ± 0.2 °C. The averaged background scattering intensity was subtracted from the raw scattering curve over the available range.

## Results and Discussion

**Phase Behavior.** ***Effect of Variation in Surfactant Amphiphilicity.*** Figure 2 shows vertical sections through the phase prisms at equal masses of EAN and dodecane for surfactants with increasing amphiphilicity: $C_8E_2$, $C_{12}E_3$, and $C_{14}E_4$. The phase behavior of $C_{10}E_2$ and $C_{10}E_3$ was also examined, but over the available temperature range $C_{10}E_2$ was present in the oil only, and $C_{10}E_3$ did not begin to phase separate until ∼80 °C, by which time impurities had begun to form in the EAN. Figure 2 is very similar to behavior reported for aqueous microemulsions (see, e.g., refs 20 and 21), and microemulsions where formamide was used as the polar solvent (see Figure 7 in ref 22). Note that the referenced papers employed octane[20,22] or decane[21] as the apolar phase, whereas for the study of EAN microemulsions, the use of dodecane was favored. The use of a heavier oil shifts $\bar{T}$ to higher temperatures, avoiding the interfacial macroemulsions that tended to occur at low temper-

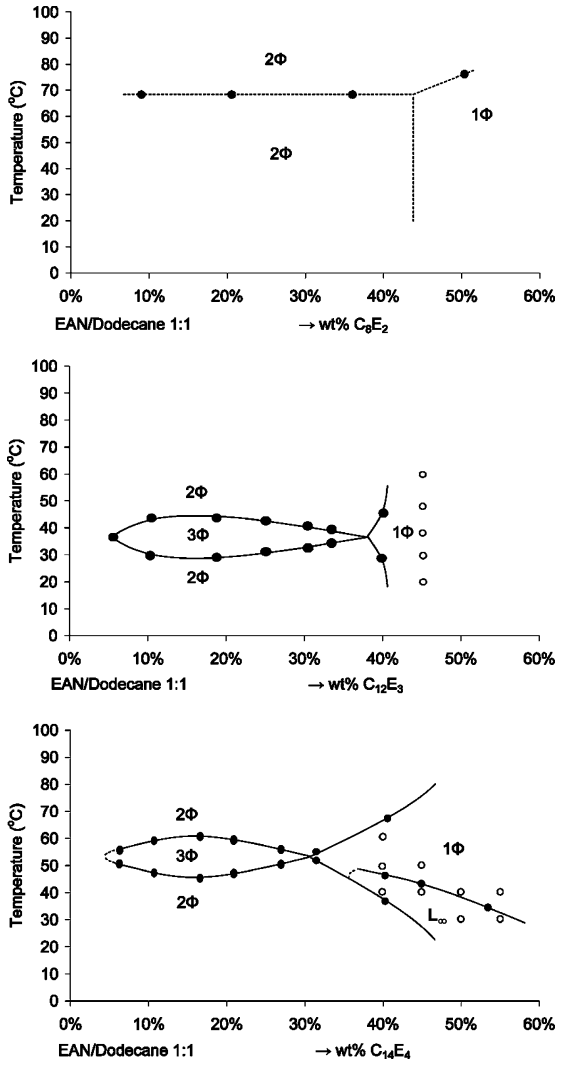


**Figure 2.** Vertical sections through the phase prisms for $C_8E_2$, $C_{12}E_3$, and $C_{14}E_4$ with equal masses of EAN and dodecane. The open circles denote samples examined by small angle X-ray scattering (Figures 6 and 7).

atures. This difference prevents direct comparison between the phase behavior of EAN microemulsions with those of water and formamide, but qualitative comparisons are still possible.

Among these EAN−dodecane−$C_iE_j$ systems, $C_8E_2$ separates into only two phases, whereas $C_{12}E_3$ forms a three phase body. This suggests that the tri-critical point[21,23] lies at amphiphilicities between those of $C_8E_2$ and $C_{12}E_3$. In water and octane the tri-critical point lies between $C_4E_0$ and$C_4E_1$,[21] and for $C_iE_j$−formamide−octane systems between $C_6E_2$ and$C_8E_3$.[22] The shift of the tri-critical point toward longer chains (higher amphiphilicity) for EAN compared to water and formamide is a consequence of two effects. First, the solvophobicity of surfactants in EAN is lower than in water, indicated by surfactant critical micelle concentrations 10−100 times higher.[5] This reduction in solvophobicity may be offset through the use of surfactants with longer hydrocarbon chains. For example, nonionic $C_iE_j$ surfactants must have hydrocarbon chains longer than $C_{12}$ to form liquid crystal phases in EAN[7] compared to longer than $C_8$ in water,[24] and the minimum chain length required to support surface hemimicelle formation at the graphite−EAN interface is $C_{16}E_j$, compared to $C_{12}E_j$ in aqueous systems.[8] Second, the use of dodecane rather than octane as the apolar phase will shift the tri-critical point toward more amphiphilic surfactants.[23]

Increasing surfactant amphiphilicity causes the fish to first grow to a maximum size and then shrink in both aqueous and formamide systems.[20−22] This decrease is identified with a change in the ternary mixture from weakly to strongly structured.[20] In water[20] this transition occurs between $C_5E_2$ and $C_6E_3$, and between $C_{10}E_4$ and $C_{12}E_4$ in formamide.[22] A similar trend is observed here. The size of the fish increases from $C_8E_2$ to $C_{12}E_3$, then decreases from $C_{12}E_3$ to $C_{14}E_4$, suggesting a change in the microemulsion from weakly to strongly structured. This is confirmed by small angle X-ray scattering and conductivity experiments as shown below. Like the tri-critical point, the transition of the weakly to strongly structured microemulsions has been displaced to higher amphiphilicities for EAN compared to water, and is consistent with reduced surfactant solvophobicity.

The surfactant efficiency (the minimum surfactant concentration required to solubilize the two immiscible solvents) increases with increasing surfactant amphiphilicity, from >45 wt % for $C_8E_2$, to ∼40 wt % for $C_{12}E_3$ and ∼30 wt % for $C_{14}E_4$. With further increase in amphiphilicity, the lamellar phase ($L_\alpha$) extends to $\bar{X}$, and a microemulsion no longer forms for either $C_{16}E_4$ or $C_{16}E_6$. The corresponding point for $C_iE_j$−water−octane systems occurs for $i = 14$, with a maximum efficiency of ∼8 wt % achieved with $C_{12}E_6$. While the use of longer oils does reduce efficiency,[23] the reduced surfactant solvophobicity in EAN is likely to be the primary reason for the lower surfactant efficiency.

*Phase Behavior as a Function of Oil Length (k).* Of the system parameters *i*, *j*, and *k*, variation in *k* is the easiest to interpret, as increasing *k* increases $T_\alpha$ while $T_\beta$ remains constant. In aqueous systems it has been shown that increasing $T_\alpha$ causes both $T_u$ and $T_l$ to increase, raising $\bar{T}$. However, $T_u$ increases somewhat faster than $T_l$, so $\Delta T$ also increases with *k*.[21] Furthermore, as $\Delta T$ increases, so to does the surfactant concentration range over which the three phase body occurs ($\Delta\gamma$), i.e., the length of the fish increases.[23]

Figure 3 shows vertical sections through the phase prism for symmetric $C_{14}E_4$−EAN−alkane systems with $k = 8$, 10, 12, and 14. The characteristics of the systems are summarized in Table 1. The same trends reported in aqueous systems[23] also occur for EAN microemulsions; $\bar{T}$ increases with *k*, from 39.5 °C for octane to 57 °C for tetradecane and the surfactant efficiency decreases with increasing *k*.[23]

The increase in $\Delta\gamma$ with increasing *k* is less marked in EAN, particularly between $k = 8$ and 10. However, the minimum surfactant concentration where the three phase body first appears and $\bar{X}$ are, to a certain extent, estimated, leading to relatively large uncertainties in $\Delta\gamma$. Nonetheless, the increase in $\Delta\gamma$ between $k = 12$ and 14 is significant and unmistakable, and in keeping with the trends observed in aqueous systems. The effect of increasing *k* on $\Delta T$ follows aqueous systems less closely. The height of the fish remains essentially constant for lighter oils, but grows for $k = 14$ (Figure 3 and Table 1). The reason for the constancy of $\Delta T$ for the lighter oils may be due to errors in the lower boundary of the three phase body (gray-shaded areas) leading to $\Delta T$ being overestimated for $k = 8$ and $k = 10$.

Phase diagrams for $C_{16}E_4$−EAN−dodecane and hexadecane are presented in Figure 4. For $k = 12$, the lamellar phase intrudes on $\bar{X}$. The presence of this $L_\alpha$ phase, coupled with the formation of a macroemulsions at various interfaces, prevented determination of the lower phase boundary and accurate identification of $\bar{X}$ for this system. Nonetheless, the upper phase boundary was determined, and a separate phase boundary within the three

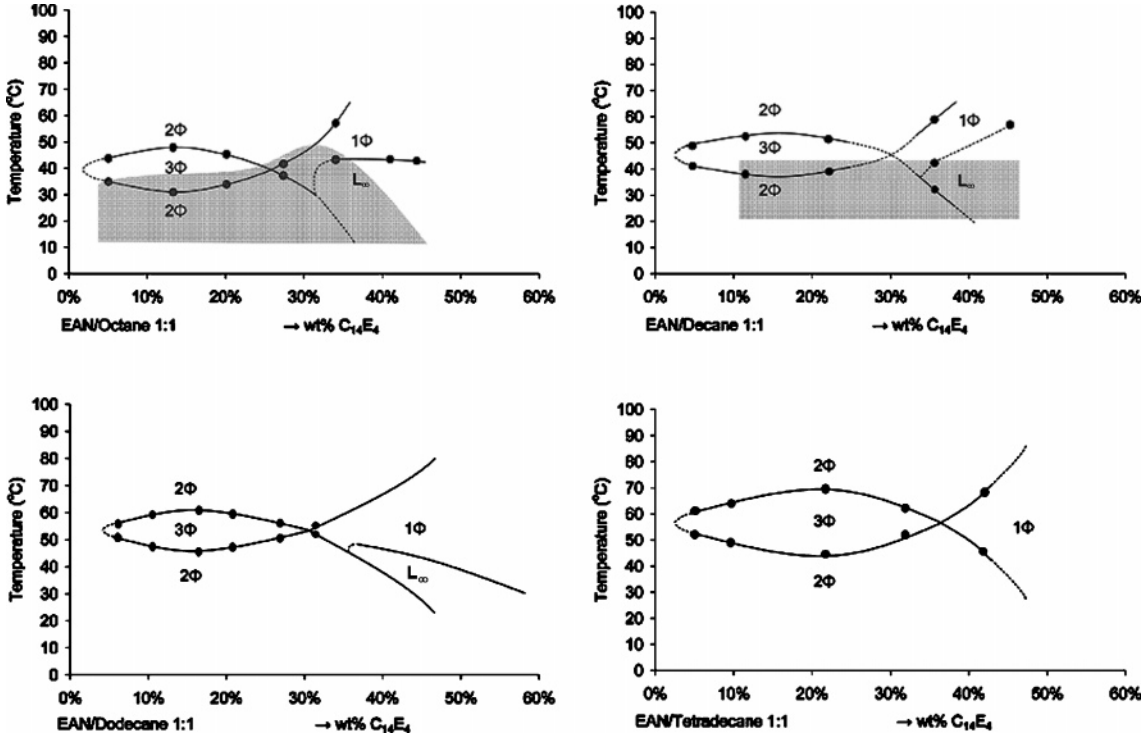


**Figure 3.** Vertical sections through the phase prisms for $C_{14}E_4$−EAN−alkane systems for $k = 8$, 10, 12, and 14 with equal masses of EAN and alkane. See the Materials and Methods section for an explanation of the gray shaded regions.

**TABLE 1: Characteristics Values for the Phase Behavior of $C_{14}E_4$−EAN−Alkane Systems**

| alkane | $T_l$ (°C) | $T_u$ (°C) | $\Delta T$ (°C) | $\bar{T}$ (°C) | $\Delta\gamma$ (wt % $C_{14}E_4$) | efficiency (wt % $C_{14}E_4$) |
|---|---|---|---|---|---|---|
| octane | 31 | 48 | 17 | 39.5 | 25 | 27 |
| decane | 37 | 54 | 17 | 45.5 | 27 | 30 |
| dodecane | 45 | 61 | 16 | 53 | 28 | 30 |
| tetradecane | 44 | 70 | 26 | 57 | 34 | 37 |

phase body identified. This boundary extends from ∼20 wt %, 40 °C toward the origin. To the right of this boundary, the middle phase is lamellar (indicated by $\leftrightarrow L_\alpha$ in the figure), whereas to the left, a typical, isotropic microemulsion phase forms. A similar situation is often observed in the one phase region in aqueous systems, where the microemulsion occurs over a narrow concentration interval between $\bar{X}$ and $L_\alpha$.[21]

The intrusion of the $L_\alpha$ phase is avoided by substitution of hexadecane for dodecane. This shifts $\bar{T}$ to higher temperatures, allowing the phase boundaries to be resolved. Despite the difficulties with the $k = 12$ system, both $\Delta\gamma$ and $\Delta T$ seem to increase between $k = 12$ and $k = 16$, and surfactant efficiency decreases with the heavier oil. These results are in line with those reported above for the $C_{14}E_4$−EAN−alkane systems, and for aqueous[23] and formamide[22] ternary mixtures.

*Phase Behavior as a Function of Headgroup Size (j).* In aqueous systems, increasing $j$ at constant $k$ and $i$ increases both $T_\alpha$ and $T_\beta$, raising $\bar{T}$. Recent studies have shown that increasing $j$ likewise raises $T_\beta$ of $C_iE_j$ surfactants in EAN. As $T_u$ rises more rapidly than $T_l$, $\Delta T$ grows larger, also accompanied by an increase in $\Delta\gamma$.[20,21] Similar behavior is thus expected in EAN.

Vertical sections through the phase prism for symmetric $C_{12}E_3$ and $C_{12}E_4$−EAN−dodecane mixtures are presented in Figure 5. The $C_{12}E_2$ system was also studied, but this surfactant remained dissolved in the dodecane down to 10 °C. $\bar{T}$ increases from 37 °C for $j = 3$ to 55 °C for $j = 4$, accompanied by an increase in $\Delta T$ from 18 to 28 °C. These results are in accordance with those for aqueous systems. However, contrary to aqueous

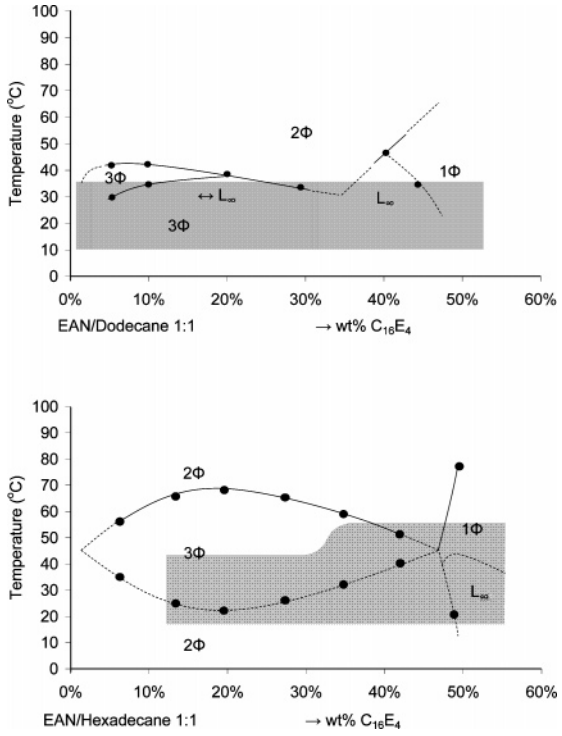


**Figure 4.** Vertical sections through the phase prisms for $C_{16}E_4$−EAN−alkane systems for $k = 12$ and 16 with equal masses of EAN and alkane. See the Materials and Methods section for an explanation of the gray shaded regions.

systems, $\Delta\gamma$ reduces with increasing $j$, while the surfactant efficiency is approximately unchanged.

*Phase Behavior as a Function of Tail Length (i).* In aqueous systems, increasing $i$ at constant $k$ and $j$ causes both $T_\alpha$ and $T_\beta$ to decrease, lowering $T_u$, $T_l$ and $\bar{T}$. $T_u$ decreases more rapidly than $T_l$, reducing $\Delta T$ and $\Delta\gamma$. Furthermore, as $i$ is increased, the $L_\alpha$ phase grows larger and draws closer to $\bar{X}$.[21]

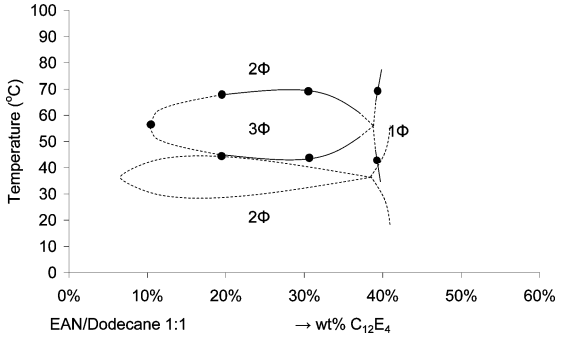


**Figure 5.** Vertical section through the phase prisms for $C_{12}E_4$−EAN−dodecane with equal masses of EAN and dodecane. The dashed outline shows the results for $C_{12}E_3$−EAN−dodecane from Figure 2.

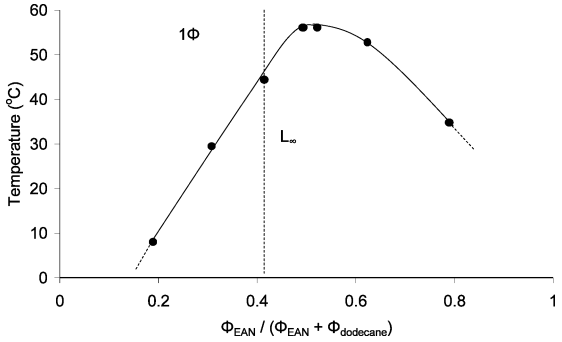


**Figure 6.** Vertical section through the phase prisms for 45 wt % $C_{14}E_4$ as a function of EAN and dodecane solvent volume fractions. Dashed vertical line indicates a 1:1 mass ratio (Figures 2 and 3).

The effect of increasing *i* on microemulsions with EAN can be ascertained by comparing $C_{12}E_4$−EAN−dodecane in Figure 5, $C_{14}E_4$−EAN−dodecane in Figure 2 and $C_{16}E_4$−EAN−dodecane in Figure 4. While no $L_\alpha$ phase is present for the $C_{12}E_4$ system, it occurs in the $C_{14}E_4$ system for surfactant concentrations slightly greater than $\bar{X}$. Further increasing *i* to 16 results in the lamellar phase increasing in size to such an extent that it dominates the phase diagram, encroaching well into the three phase body, preventing determination of the characteristic values for this system. As *i* increases from 12 to 14, both $\bar{T}$ and $\Delta T$ decrease in accordance with results for aqueous systems. No trend can be ascertained for $\Delta\gamma$, which remains fairly constant across the three hydrocarbon chain lengths examined.

*Phase Behavior as a Function of the EAN:Dodecane Ratio.* Figure 6 shows the lamellar to microemulsion transition temperature on a vertical section through the phase prism parallel to the EAN−dodecane axis at 45 wt % $C_{14}E_4$. This may be compared to similar figures in refs 21 and 25. It should be noted, however, that this section is situated farther from $\bar{X}$, and consequently, two phase regions are not observed over the temperature range examined.

The $L_\alpha$ phase is most stable as a function of temperature when the EAN and dodecane volume fractions are equal. We postulate that this may be a consequence of the surfactant monolayers at internal oil/EAN interfaces being most weakly coupled in the equal solvent volume system, where they are farthest apart. If the solvent volume fractions are not equal, either the surfactant headgroups or the tails in neighboring monolayers are in closer proximity, which will damp membrane undulations. Therefore, the equal volume system has the greatest tolerance for the increasing level of fluctuations[26−36] in the $L_\alpha$ surfactant layers as temperature is raised. Damping fluctuations thus raises the free energy of the planar monolayer, and favors a non-preferred curvature.[37] In addition to these considerations, droplets are entropically favored at high solvent ratios: when oil is present in excess, reverse micelles swollen with EAN form, whereas when EAN is the greater volume fraction, oil-swollen direct micelles result. The microstructures associated with this phase diagram are discussed further below.

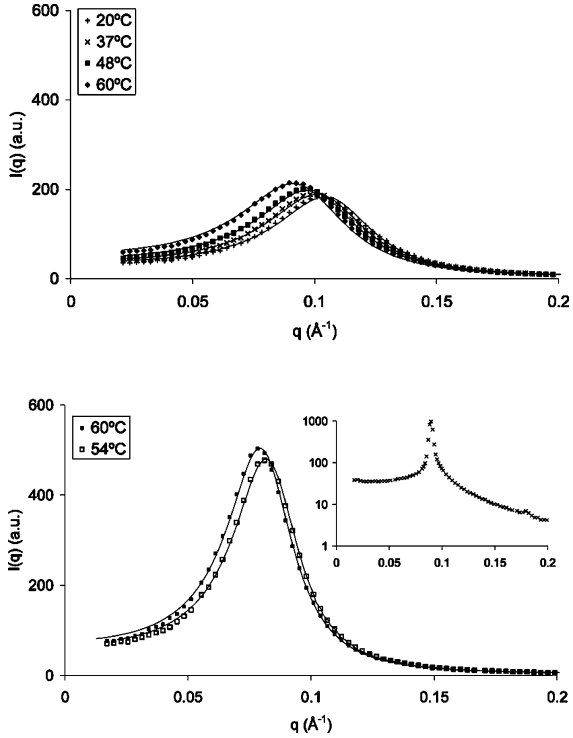


**Figure 7.** Top: Small-angle X-ray spectra for 45 wt % $C_{12}E_3$−EAN−dodecane (top) and 40 wt % $C_{14}E_4$−EAN−dodecane (bottom) as a function of temperature. The inset shows first and second-order reflections of the $L_\alpha$ spectrum of $C_{14}E_4$−EAN−dodecane at 40 °C on a logarithmic scale. For both surfactants the solid lines show fits using the Teubner−Strey model (see text).

**Microstructure of the Microemulsion and Lamellar Phases.** SAXS spectra of symmetric 45 wt % $C_{12}E_3$−EAN−dodecane and 40 wt % $C_{14}E_4$−EAN−dodecane systems as a function of temperature are presented in Figure 7. A single, broad scattering peak is observed at all temperatures for the $C_{12}E_3$ system, like that observed in aqueous microemulsions.[25] The $C_{14}E_4$ system behaves similarly above 40 °C, but shows 2 orders of diffraction at and below 40 °C, consistent with the position of the $L_\alpha$ phase boundary shown in Figure 2.

The greater peak width for the $C_{12}E_3$ system compared to the $C_{14}E_4$ system suggests it is less ordered, consistent with the absence of a lamellar phase (see below). The relative widths of the microemulsion peaks of both systems (normalized to peak position and intensity, $q_{max}$ and $I_{max}$) also increased as the temperature was increased, indicating decreasing order.

The peak position in both microemulsions decreases monotonically as temperature is increased, indicating an increase in the characteristic length scale of the system, and a decrease in the internal surface area. This may arise from simple effects such as higher solubility of the surfactant in oil and/or EAN at higher temperatures, or to increases in the molar volumes of the oil and EAN, both of which would reduce the amount of surfactant available to stabilize internal interfaces. In the $C_{12}E_3$ system the peak decreases from 0.1 $Å^{-1}$ at 20 °C to 0.088 $Å^{-1}$ at 60 °C, corresponding to a 14% increase in repeat spacing. Even in a bilayer-based structure, this is too much to be accounted for by the small changes in molar volume of EAN (1.5%)[38] or dodecane (4%)[39] over a 40 °C range. Although the

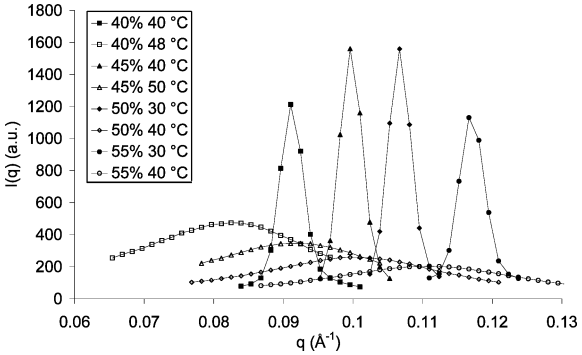


**Figure 8.** Partial small-angle X-ray scattering spectra of symmetric $C_{14}E_4$−EAN−dodecane mixtures as a function of surfactant concentrations at temperatures straddling the $L_\alpha$−microemulsion phase boundary. Spectra in the $L_\alpha$ phaseare represented by full symbols and the microemulsion phase by open symbols. The surfactant concentration is given in the legend. The lines are to guide the eye for the $L_\alpha$ phase and fits using the Teubner-Strey model for the microemulsion phase.

solubility of the surfactant in the oil will increase by a few percent over a similar temperature range, the existence of cloud points suggests that the solubility in EAN will decrease, if anything, and therefore cannot account for the observed change in peak position.

The cloud point also means that the area occupied by polyoxyethylene groups in contact with EAN should decrease as the temperature is increased.[36] Provided that the volume fraction of the interfacial surfactant layer does not vary with temperature,[40,41] this lowers the membrane surface area and produces larger droplets. Excess interfacial area may also be stored in membrane undulations as the level of thermal fluctuations increases with temperature,[33] reducing the effective internal interfacial area. These effects are currently being investigated by neutron scattering of EAN microemulsions using isotopic substitution to yield bulk and film contrast.

Small-angle X-ray scattering curves for the symmetric $C_{14}E_4$−EAN−dodecane system are presented in Figure 8 as a function of surfactant concentration at temperatures that straddle the $L_\alpha$−microemulsion phase boundary within the "fish tail" (cf. Figure 2). The form of the data is strikingly similar to that reported for the $C_{12}E_5$−water−octane system.[25] In both the aqueous and EAN systems, a sharp, intense peak is observed in the $L_\alpha$ region. Upon increasing temperature the phase boundary is crossed and the peak becomes broader, less intense and shifts to lower $q$, indicating that both the characteristic length and disorder of the system have increased.

In comparable aqueous lamellar phases,[25,42] the repeat spacing $D^* = 2\pi/q_{max}$ varies inversely with surfactant concentration according to[25]

$$a_s = \frac{2v_s}{D^*\Phi_s} \quad (1)$$

where $a_s$ is the area occupied by the surfactant, $\Phi_s$ is the volume fraction of surfactant, and the molecular volume of the amphiphile molecule $v_s = M\rho_s^{-1}N_a^{-1}$ is determined from the surfactant density ($\rho_s$) and molecular weight ($M$). Table 2 shows that $a_s = 48.3 \pm 1.2$ Å$^2$ thus calculated for these $C_{14}E_4$−EAN−dodecane lamellar phases is constant within experimental uncertainty, indicating that one-dimensional swelling is responsible for the shift in the position, just as in aqueous systems.

This system most closely resembles $C_{12}E_5$−water−octane in its phase behavior and scattering; The microemulsion peaks become broader and move to higher $q$ with increasing surfactant concentration and consequent decrease in domain size.[24,43−49] However, the aqueous lamellar phase has a much smaller molecular area of $a_s = 42.9$ Å$^2$.[25] As the oil does not influence $a_s$,[50] the effective size of the $E_4$ headgroup is greater in EAN than $E_5$ in water.[51] We attribute this to the fact that the ethylammonium ion that hydrogen bonds to the surfactant headgroup in EAN and its nitrate counterion are much larger than a water molecule, producing an increased area of steric interaction.

**TABLE 2: $D^*$, $q_{max}$ and $a_s$ for the $L_\alpha$ Phase of $C_{14}E_4$−EAN−Dodecane at Various Surfactant Volume Fractions[a]**

| $\Phi_s$ | T (°C) | $q_{max}$ (Å$^{-1}$) | $D^*$ (Å) | $a_s$ (Å$^2$) |
|---|---|---|---|---|
| 0.40 | 40 | 0.09 | 71 | 50 |
| 0.45 | 40 | 0.10 | 63 | 49 |
| 0.50 | 30 | 0.11 | 59 | 47 |
| 0.55 | 30 | 0.12 | 54 | 47 |

[a] Note that the densities of $C_{14}E_4$,EAN and dodecane are such that the surfactant mass and weight fractions are essentially equal.

**TABLE 3: $D^*$ and $a_s$ for the $L_\alpha$ Phase for Various EAN:dodecane Ratios with 45 wt % $C_{14}E_4$ at 20 °C[a]**

| EAN (g) | dodecane (g) | $\Phi_{EAN}/(\Phi_{EAN} + \Phi_{dodecane})$ | $\Phi_s$ | $D^*$ (Å) | $a_s$ (Å$^2$) |
|---|---|---|---|---|---|
| 0.20 | 0.35 | 0.26 | 0.43 | 63 | 54 |
| 0.25 | 0.30 | 0.34 | 0.44 | 63 | 51 |
| 0.28 | 0.28 | 0.38 | 0.45 | 62 | 51 |
| 0.30 | 0.25 | 0.43 | 0.45 | 61 | 51 |
| 0.35 | 0.20 | 0.52 | 0.47 | 57 | 54 |
| 0.40 | 0.15 | 0.62 | 0.48 | 57 | 52 |

[a] $\Phi_{EAN}$ and $\Phi_{dodecane}$ represent the volume fractions of EAN and dodecane, respectively.

SAXS spectra were recorded in the $L_\alpha$ phase at 20 °C for 45 wt % $C_{14}E_4$ at various dodecane and EAN compositions shown in Figure 6. Repeat spacings (Table 3) decrease as the fraction of EAN in the system is increased simply because of the greater density of EAN (1.21 mg mL$^{-1}$ versus 0.75 mg mL$^{-1}$), which increases $\Phi_s$. The molecular area (eq 1) remains essentially constant at $52.2 \pm 1.5$ Å$^2$ for all EAN to dodecane ratios, which is slightly greater than the values determined at higher temperatures (Table 2).

In the microemulsion phase at 60 °C, a single broad scattering peak occurs, as shown in Figure 9 (top). A maximum in both the characteristic length scale and scattered intensity are observed at equal volumes of EAN and dodecane, also shown in Figure 9, in accordance with results for aqueous systems.[25,44,46,48] Critically, the value of $a_s$ calculated from D* varies considerably for these microemulsion systems, discounting the possibility of a distorted $L_\alpha$ arrangement for the microemulsion phase.

SAXS spectra from EAN microemulsions were fitted to the Teubner−Strey model,[42,49,52] which has been widely used to describe scattering from aqueous microemulsions stabilized by nonionic surfactants. This model uses three fitting parameters to describe the observed broad scattering peak and $q^{-4}$ decay at large $q$ in terms of two lengths; the periodicity of the oil and water domains, $d$, and a correlation length, $\xi$, which describes the decay of that periodic order. The scattering function has the form[50]

$$I(q) = \frac{A}{1 + Bq^2 + Cq^4} \quad (2)$$

The Teubner−Strey model yields excellent fits to the SAXS

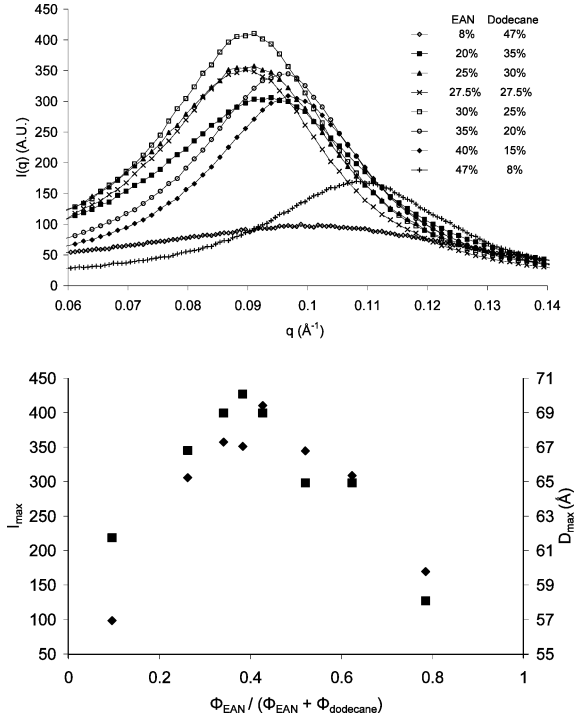


**Figure 9.** Top: SAXS spectra at constant 45 wt % $C_{14}E_4$ at 60 °C with varying masses of EAN and dodecane, as indicated in the Figure legend. Lines are to guide the eye. Bottom: (◆) $I_{max}$ and (■) characteristic length, $D^* = 2\pi/q_{max}$.

**TABLE 4: Values of the Periodicity *d* and Correlation Length $\xi$ Derived from Teubner−Strey Fits for Various Symmetric EAN Microemulsions Near $\bar{X}$**

| $C_iE_j$ | oil | $C_iE_j$ (wt %) | $T$ (°C) | $d$ (Å) | $\xi$ (Å) | $d/\xi$ |
|---|---|---|---|---|---|---|
| $C_{12}E_3$ | dodecane | 45 | 37 | 61 | 41 | 1.49 |
| $C_{14}E_4$ | octane | 45 | 40 | 60 | 63 | 0.95 |
| $C_{14}E_4$ | dodecane | 40 | 54 | 75 | 61 | 1.23 |
| $C_{14}E_4$ | dodecane | 45 | 50 | 67 | 61 | 1.10 |
| $C_{14}E_4$ | dodecane | 50 | 50 | 61 | 58 | 1.05 |
| $C_{14}E_4$ | dodecane | 55 | 50 | 55 | 56 | 0.98 |
| $C_{14}E_4$ | hexadecane[a] | 45 | 60 | 69 | 51 | 1.35 |
| $C_{16}E_4$ | dodecane[b] | 50 | 60 | 80 | 74 | 1.08 |
| $C_{16}E_4$ | hexadecane | 50 | 50 | 66 | 63 | 1.05 |

[a] The phase diagram for this system was not determined. The position of $\bar{X}$ is estimated. [b] This sample is at a temperature greater than $\bar{T}$, as a $L_\alpha$ phase is present at $\bar{T}$ (Figure 4).

spectra of $C_iE_j$−EAN−alkane systems shown in Figures 7 and 8. Values of $d$ and $\xi$ for various balanced microemulsions close to $\bar{X}$ are presented in Table 4. Both fitted parameters are much smaller than those typically observed in balanced aqueous microemulsions near their $\bar{X}$ point, as the surfactant efficiency in EAN systems is so much less. Higher interfacial area necessitates smaller domains. In aqueous microemulsions both $d$ and $\xi$ decrease with increasing surfactant concentration.[50] Table 4 shows that the same trend occurs in $C_{14}E_4$−EAN−dodecane microemulsions as the surfactant concentration is increased from 40 to 55 wt %.

A survey of balanced aqueous $C_iE_j$ microemulsions with $8 \le i \le 12$, $3 \le j \le 6$ and various alkanes $8 \le k \le 14$ has yielded the general result that $d \approx 2\xi$ close to $\bar{X}$, provided a correction is made for the mass of surfactant monomer dissolved in the water and oil phases.[50] That is, the correlation length of these microemulsions is about the same as the size of the oil or water domains.

In EAN microemulsions, we find $d \approx \xi$ for most systems studied. This implies that polar and apolar domains remain correlated across more internal interfaces, and that EAN microemulsions are more highly structured than corresponding aqueous systems. This is partly a necessary consequence of the lower surfactant efficiency in EAN, combined with higher area per molecule than aqueous systems. In aqueous microemulsions, $d/\xi$ decreases with increasing surfactant concentration, but does not approach unity at the same surfactant concentrations. Small-angle neutron scattering experiments are under way to investigate this further.

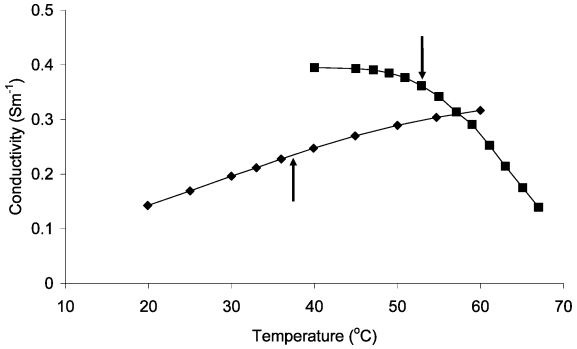


**Figure 10.** Electrical conductivity of symmetric EAN/dodecane microemulsions as a function of temperature. (◆) 45 wt % $C_{12}E_3$ and (■) 40 wt % $C_{14}E_4$. Lines are to guide the eye, and arrows denote $\bar{T}$.

In aqueous systems, as $i$ is increased at constant $j$ and $k$, $\xi$ increases logarithmically.[50] A similar trend is found in $C_{14}E_4$−EAN−dodecane and $C_{16}E_4$−EAN−dodecane systems, where both $d$ and $\xi$ increase as the surfactant tailgroup is lengthened. In aqueous microemulsions, $\xi$ decreases as the length of the oil is increased.[50] Table 4 shows a similar trend for EAN microemulsions, with $d$ and $\xi$ decreasing for $C_{16}E_4$ as the oil is changed from dodecane to hexadecane. The values of $d$ and $\xi$ listed for the octane systems are for temperatures greater than $\bar{T}$, due to the extensive $L_\alpha$ phase, but as smaller structures are expected at temperatures greater than $\bar{T}$, this result is in keeping with observations made in aqueous systems. However, the results for $C_{14}E_4$ and EAN with octane, dodecane and hexadecane do not follow the aqueous trend, with $d$ and $\xi$ both increasing with increasing $k$. As $\bar{T}$ increases with $k$, this may be a consequence of the loss of interfacial area at constant surfactant concentration, which occurs as the temperature is increased.

In aqueous systems, a maximum in the size of the three phase fish body has been correlated with a change in the microstructure with amphiphilicity from weakly to strongly structured.[20] In EAN microemulsions this occurs between $C_{12}E_3$ and $C_{14}E_4$ (Figure 2). The scattering peak for the balanced $C_{12}E_3$−EAN−dodecane system is much broader and less intense than the $C_{14}E_4$−EAN−dodecane system (Figure 7), suggesting that the $C_{12}E_3$ system is more weakly structured. The $C_{12}E_3$ system has the largest $d/\xi$ value of all microemulsion examined, also suggesting that it is less well-structured than other EAN microemulsions.

In strongly ordered aqueous microemulsions (with a small amount of added electrolyte), electrical conductivity decreases as the microstructure changes from water continuous or bicontinous to oil continuous. Conductivity results for $C_{14}E_4$−EAN−dodecane microemulsions (Figure 10) are typical of such a strongly structured microemulsion.[53] The decrease in conductivity with increasing temperature indicates that the EAN solvent becomes discontinuous (oil continuous) at higher temperatures, falling away above $\bar{T}$. In contrast, the conductivity of the $C_{12}E_3$−EAN−dodecane system increases over the entire temperature range, and $\bar{T}$ does not correspond to any particular feature.

## Conclusions

The phase behavior and microstructure of ternary mixtures of nonionic $C_iE_j$ surfactants, alkanes and the ionic liquid EAN closely parallels observations in water. In general, the surfactant chain length must be ~4−6 $CH_2$ groups longer in EAN to produce effects similar to those observed in aqueous systems such as a strongly structured microemulsion or an intruding lamellar phase.

Increasing the amphiphilicity initially increases, and then decreases, the dimensions of the "fish" body. As the fish begins to decrease in size, the microemulsions undergo transition from weakly to strongly structured. For EAN−dodecane systems, this occurs between $C_{12}E_3$ and $C_{14}E_4$, as shown using both SAXS and conductivity. EAN microemulsions responded to changes in the length of the surfactant headgroup, tail and alkane in a manner broadly consistent with aqueous systems. A lamellar phase was often present at lower temperatures for surfactants with longer alkyl tails. Variation in the dodecane to EAN ratio for constant surfactant concentration revealed that this phase had the highest melting point when the solvent volumes were equal.

Where present, lamellar phases followed the expected one-dimensional swelling behavior with surfactant concentration at constant molecular area. The effective area of interaction for each ethoxy unit was found to be significantly higher in EAN than water. This is attributed to the increased size of the species that hydrogen bond to the headgroup in the ionic liquid (ethylammonium, nitrate) compared to water.

In microemulsion phases a single broad scattering peak was observed reminiscent of aqueous systems. This microemulsion peak was modeled using the Teubner−Strey model. The values of $d$ and $\xi$ indicate that EAN microemulsions are generally more highly structured than their aqueous counterparts. For the most part, variation in the length of the surfactant tailgroup and alkane oil produced changes in $d$ and $\xi$ consistent with aqueous systems.

Both the lamellar and microemulsion scattering peaks shifted to lower $q$ as the temperature is increased above $T$. This is due to a decrease in the interfacial area of the surfactant layer as temperature is increased, a consequence of the increased level of thermal fluctuations and the lower area of interaction of the surfactant headgroup with EAN.

**Acknowledgment.** We thank Tracey Hanley and Annabelle Blom for their assistance with the SAXS experiments, Liliana DeCampo for her assistance with the analysis and modeling of the SAXS data, and Alex Djerdjev for his help collecting the conductivity data. This work was supported by the Australian Research Council, and R.A. acknowledges receipt of an ARC Postdoctoral Fellowship.

## References and Notes

(1) Forsyth, S. A.; Pringle, J. M.; MacFarlane, D. R. *Aust. J. Chem.* **2004**, *57*, 113.
(2) Rodgers, R. D.; Seddon, K. R. *Science* **2003**, *302*, 792.
(3) Seddon, K. R.; Stark, A.; Torres, M.-J. *Pure Appl. Chem.* **2000**, *72*, 2275.
(4) Wenton, T. *Chem. Rev.* **1999**, *99*, 2071.
(5) Evans, D. F.; Yamauchi, A.; Roman, R.; Casassa, E. Z. *J. Colloid Interface Sci*. **1982**, *88*, 89.
(6) Evans, D. F.; Yamauchi, A.; Wei, G. J.; Bloomfield, V. A. *J. Phys. Chem*. **1983**, *87*, 3537. Bowlas, C. J.; Bruce, D. W.; Seddon, K. R. *Chem. Commun*. **1996**, 1625. Gordon, C. M.; Holbrey, J. D.; Kennedy, A. R.; Seddon, K. R. *J. Mater. Chem*. **1998**, *8*, 2627. Firestone, M. A.; Dzielawa, J. A.; Zapol, P.; Curtiss, L. A.; Seifert, S.; Dietz, M. L. *Langmuir* **2002**, *18*, 7258. Yoshio, M.; Mukai, T.; Kanie, K.; Yoshizawa, M.; Ohno, H.; Kato. T. *Adv. Mater*. **2002**, *14*, 351. Anderson, J.L.; Pino, V.; Hagberg, E.C.; Sheares, V.V.; Armstrong, D.W. *Chem. Commun*. **2003**, 2444. Yoshio, M.; Mukai, T.; Kanie, K.; Yoshizawa, M.; Ohno, H.; Kato, T. *Chem. Lett.* **2002**, 320. Fletcher, K. A.; Pandey, S. *Langmuir* **2004**, *20*, 33.
(7) Araos, M. U.; Warr, G. G. *J. Phys. Chem. B*. **2005**, *109*, 14275.
(8) Atkin, R.; Warr, G. G. *J. Am. Chem. Soc.* **2005**, *34*, 11940.
(9) Beesley, A. H.; Evans, D. F.; Laughlin R. G.; *J. Phys. Chem.* **1988**, *92*, 791−793.
(10) Hunter, R. J. *Foundations of Colloid Sciencel*; Oxford University Press: Oxford, U.K., 1985.
(11) Auvray, L.; Cotton, J. P.; Ober, R.; Taupin, C. *J. Phys. Chem.* **1984**, *88*, 4586. Jahn, W.; Strey, R.; *J. Phys. Chem.* **1988**, *92*, 2294.
(12) Gennes, P G.; Taupin, C. *J. Phys. Chem.* **1982**, *86*, 2294.
(13) Helfrich, W.; Naturforsch, Z. *Teil A.* **1978**, *33*, 305.
(14) Kahlweit, M;. Strey, R.; Firman, P.; Haase, D.; Jen, J.; Schomacker, R. *Langmuir* **1988**, *4*, 499.
(15) Gao, H. X.; Li, J. C.; Han, B. X; Chen, W. N.; Zhang, J. L.; Zhang R.; Yan, D. D. *Phys. Chem. Chem. Phys*. **2004**, *6*, 2914.
(16) Eastoe, J.; Gold, S.; Rogers, S. E.; Paul, A.; Welton, T.; Heenan, R. K.; Grillo, I. *J. Am. Chem. Soc*. **2005**, *127*, 7302.
(17) Gao, Y.; Han, S.; Han, B.; Li, G.; Shen, D.; Li, Z.; Du, J.; Hou, W.; Zhang, G. *Langmuir* **2005**, *21*, 5681.
(18) Gao, Y.; Li, N.; Zheng, L.; Zhao, X.; Zhang, S.; Han, B.; Hou, W.; Li, G. *Green Chem.* **2006**, *8*, 43.
(19) Kahlweit, M.;. Strey, R.; Busse, G. *Phys. Chem.* **1990**, *94*, 3881.
(20) Kahlweit, M.;. Strey, R.; Busse, G. *Phys. Rev. E* **1993**, *47*, 4197.
(21) Kahlweit, M.;. Strey, R.; Firman, P. *J. Phys. Chem.* **1986**, *90*, 671.
(22) Schubert, K. V.; Busse, G.; Strey, R.; Kahlweit, M. *J. Phys. Chem*, **1993**, *97*, 248.
(23) Kahlweit, M.;. Strey, R.; Firman, P. J, Haase, D. *Langmuir*, **1985**, *1*, 281.
(24) Penders, M. H. G. M.; Strey, R. *J. Phys. Chem.* **1995**, *99*, 6091.
(25) Lichterfeld, F.; Schmeling, T.; Strey, R. *J. Phys. Chem.* **1986**, *90*, 5762.
(26) Helfrich, W. *Z. Naturforsch.* **1978**, *33a*, 305.
(27) Larche, F. C.; Appell, J.; Porte, G.; Bassereau, P.; Marignan, J. *Phys. Rev. Lett.* **1986**, *56*, 1700.
(28) Safinya, C. R.; Roux, D.; Smith, G. S.; Sinha, S. K.; Dimon, P.; Clark, N. A.; Bellocq, A.-M. *Phys. Rev. Lett.* **1986**, *57*, 2718.
(29) Bassereau, P.; Marignan, J.; Porte, G.; May, R. *Europhys. Lett.* **1991**, *15*, 753.
(30) Nallet, F.; Roux, D.; Milner, S. T. *J. Phys. (Paris*) **1990**, *51*, 2333.
(31) Roux, D.; Cates, M. E.; Olsson, U.; Ball, R. C.; Nallet, F.; Bellocq, A.-M. *Europhys. Lett.* **1990**, *11*, 753.
(32) Di, Meglio, J.-M.; Bassereau, P. *J. Phys. II* **1991**, *1*, 247.
(33) Roux, D.; Nallet, F.; Freyssingeas, E.; Porte, G.; Bassereau, P.; Skouri, M.; Marignan, J. *Europhys. Lett.* **1992**, *17*, 575.
(34) Halle, B.; Quist, P.-O. *J. Phys. II* **1994**, *4*, 1823.
(35) Auguste, F.; Barois, P.; Fredon, L.; Clin, B.; Dufourcq, E. J.; Bellocq, A.-M. *J. Phys, II* **1994**, *4*, 2197.
(36) Freyssingeas, É.; Nallet, Roux, F., D. *Langmuir* **1996**, *12*, 6028.
(37) Mitchell, J. D.; Tiddy, G. J. T.; Waring, L.; Bostock, T.; McDonald, M. P. *J. Chem. Soc., Faraday Trans. II* **1983**, *79*, 975.
(38) Allen, M.; Evans, D. F.; Lumry, R.; *J. Solution Chem.* **1985**, 14, 549.
(39) *CRC Handbook of Chemistry and Physics*; Lide, D. R., Ed.; CRC Press: Boca Raton, FL, 1998.
(40) Strey, R. *Colloid Polym. Sci*. **1994**, *272*, 1005.
(41) Luzzati, V.; Mustacchi, H.; Skoulios, A.; Husson, F. *Acta Crystallogr*. **1960**, *13*, 660. Luzzati, V.; Mustacchi, H.; Husson, F. *Acta Crystallogr*. **1960**, *13*, 668.
(42) Ekwall, P. In *Advances in Liquid Crystals*; Brown, G. H., Ed.; Academic Press: St. Louis, MO, 1975; Vol. 1.
(43) Araos M.; Warr G. G. in preparation.
(44) Cebula, D. J.; Ottewill, R. M.; Ralston, J. Pusey, P. N. *J. Chem. Soc. Faraday Trans. 1* **1981**, *77*, 2585.
(45) Auvary, L.; Cotton, J. P.; Ober, R.; Taupin, C. *J. Phys. Chem.* **1984**, *88*, 4586.
(46) Auvary, L.; Cotton, J. P.; Ober, R.; Taupin, C. *J. Phys.* **1984**, *45*, 913.
(47) Kotlarchyk, M.; Chen, H. S.; Huang, J. S.; Kim, M. W. *Phys. Rev. Lett.* **1984**, *53*, 941.
(48) De Geyer, A.; Tabony, J. *Chem. Phys. Lett.* **1985**, *113*, 83.
(49) Teubner, M.; Strey, R. *J. Chem. Phys.* **1987**, *87*, 3195.
(50) Sottmann, T.; Strey, R.; Chen, S.-H. *J. Chem. Phys.* **1997**, *106*, 6483.
(51) Paz, L.; Di Meglio, J. M.; Dvolaitzky, M.; Ober, R.; Taupin, C. *J. Phys. Chem.* **1984**, *88*, 3415.
(52) Chen, S.-H.; Chang, S.-l.; Strey, R. *Prog. Colloid Polym. Sci.* **1990**, *81*, 30.
(53) Sottmann, T.; Stey, R. In *Fundamentals of Interface and Colloid Science*; Lyklema, J. Ed.; Academic Press: St. Louis, MO, **2005**; Vol 5.